GENERAL ARTICLE

Molecular mechanism for the multiple sclerosis risk variant rs17594362

Dongkyeong Kim and Yungki Park*

Department of Biochemistry, Jacobs School of Medicine and Biomedical Sciences, Hunter James Kelly Research Institute, State University of New York at Buffalo, Buffalo, NY 14203, USA

*To whom correspondence should be addressed. Tel: +1 7168817579; Fax: 1 7168496651; Email: yungkipa@buffalo.edu

Abstract

Multiple sclerosis (MS) is known as an autoimmune demyelinating disease of the central nervous system. However, its cause remains elusive. Given previous studies suggesting that dysfunctional oligodendrocytes (OLs) may trigger MS, we tested whether single nucleotide polymorphisms (SNPs) associated with MS affect OL enhancers, potentially increasing MS risk by dysregulating gene expression of OL lineage cells. We found that two closely spaced OL enhancers, which are 3 Kb apart on chromosome 13, overlap two MS SNPs in linkage disequilibrium—rs17594362 and rs12429256. Our data revealed that the two MS SNPs significantly up-regulate the associated OL enhancers, which we have named as Rgcc-E1 and Rgcc-E2. Analysis of Hi-C data and epigenome editing experiments shows that Rgcc is the primary target of Rgcc-E1 and Rgcc-E2. Collectively, these data indicate that the molecular mechanism of rs17594362 and rs12429256 is to induce Rgcc overexpression by potentiating the enhancer activity of Rgcc-E1 and Rgcc-E2. Importantly, the dosage of the rs17594362/rs12429256 risk allele is positively correlated with the expression level of Rgcc in the human population, confirming our molecular mechanism. Our study also suggests that Rgcc overexpression in OL lineage cells may be a key cellular mechanism of rs17594362 and rs12429256 for MS.

Introduction

Multiple sclerosis (MS) is known as an autoimmune demyelinating disease of the central nervous system (1–3). However, its cause remains elusive. There are two competing hypotheses for the etiology of MS (4–8). The 'outside-in' hypothesis posits that a primary dysregulation of the immune system triggers autoimmunity against myelin, leading to demyelination and neurological deficits. Alternatively, the 'inside-out' hypothesis entertains the idea that dysfunctional OLs initiate demyelination and/or OL death, secondarily inducing autoimmunity against myelin. Given the heterogeneity of pathology observed in MS lesions, both hypotheses may be relevant. To gain insight into MS etiology, the International MS Genetics Consortium has conducted a large-scale genome-wide association study (GWAS), identifying 102 single nucleotide polymorphisms (SNPs) associated with MS (9). Most MS SNPs are mapped to non-coding regions of the genome, and it is unclear how they confer genetic risk for MS. In order to translate the MS GWAS findings into the development of novel therapies, it is absolutely necessary to decode the functional mechanisms of the 102 MS SNPs.

Studies in other fields have shown that disease SNPs in non-coding regions tend to act by impairing enhancers, dysregulating gene expression of disease-relevant cell types (10–13). We hypothesized that the same may be true for the MS SNPs. More specifically, we asked whether the MS SNPs impinge on OL enhancers, modestly dysregulating the gene expression of OL lineage cells. This modest dysregulation may not have an

outright impact on developmental myelination because it is so robust, yet over time its accumulated effect could significantly perturb the integrity of OLs, especially in a vulnerable condition that depends on genetic background and environmental exposure. The compromised integrity of OLs may then make it more prone for the immune system to develop autoimmunity against myelin, initiating the vicious cycle of demyelination, release of more antigenic molecules and stronger subsequent autoimmunity.

To probe a potential link between the 102 MS SNPs and OL enhancers, we have constructed a genome-wide map of putative OL enhancers by analyzing public OL ChIP-seq data (14). This map uncovered nine putative OL enhancers that overlap eight MS SNPs or SNPs in linkage disequilibrium with them. We found that two of the nine putative OL enhancers are bona fide OL enhancers that are active in the human brain. The two OL enhancers, which are 3 Kb apart on chromosome 13, are associated with rs17594362 (a tagging SNP for the MS GWAS (9)) and rs12429256 (in linkage disequilibrium with rs17594362, $r^2 = 1$). In each case, the MS SNP significantly upregulated the associated OL enhancer in both proliferating and differentiating OL precursor cells (OPCs). Our interdisciplinary analysis revealed that Rgcc (also known as Rgc-32) is the primary target of the two OL enhancers. This is why we have named the OL enhancers as Rgcc-E1 (overlapping rs17594362) and Rgcc-E2 (overlapping rs12429256). Taken together, the main effect of rs17594362 and rs12429256 is to increase Rgcc expression by potentiating the enhancer activity of Rgcc-E1 and Rgcc-E2, which was confirmed by the expression quantitative trait loci (eQTL) analysis of the GTEx project (15). Our study also suggests that Rgcc overexpression in OL lineage cells may be a key cellular mechanism of rs17594362 and rs12429256 for MS.

Results

Two closely spaced OL enhancers overlap two MS SNPs in linkage disequilibrium

To study the role of OL enhancers in development and disease, we have constructed a genome-wide map of 21 324 putative OL enhancers by analyzing public OL ChIP-seq data (14). We compared this map with the 102 SNPs identified by the International MS Genetics Consortium as being significantly associated with MS (9) and SNPs in linkage disequilibrium with them. This comparison revealed 9 putative OL enhancers that overlap 8 MS SNPs or SNPs in linkage disequilibrium with them: rs17594362 (Vwa8 [the nearest gene]), rs12429256 (Vwa8), rs1335532 (CD58), rs17174870 (MERTK), rs4285028 (SLC15A2), rs2303759 (DKKL1), rs307896 (SAE1), rs12212193 (BACH2) and rs4902647 (ZFP36L1). There are two points to be noted about the genome-wide map of putative OL enhancers. First, the OL ChIP-seq data that we analyzed for the genome-wide map of putative OL enhancers are all from cultured rat OL lineage cells. Second, to minimize false negatives in predicting OL enhancers, we applied rather lenient criteria to the analysis of the OL ChIP-seq data. Consequently, some of the putative OL enhancers in our map may not be operative in the human central nervous system. To determine whether the nine putative OL enhancers associated with the MS SNPs are bona fide OL enhancers that are active in the human brain, we looked up the H3K27ac ChIP-seq data from the NIH Roadmap Epigenomics Project (16). The Roadmap Epigenomics Project performed ChIP-seq experiments on human tissues for several histone marks, including H3K27ac that is associated

with active enhancers (17). The Roadmap Epigenomics Project H3K27ac ChIP-seq data show that two putative OL enhancers associated with rs17594362 (a tagging SNP for the MS GWAS (9)) and rs12429256 (in linkage equilibrium with rs17594362, $r^2 = 1$) overlap strong brain-specific H3K27ac peaks (Fig. 1). This observation suggests that these two putative OL enhancers, which are 3 Kb apart on chromosome 13, are bona fide OL enhancers that are active in the human brain. For a reason to be explained later, we have named them as Rgcc-E1 (overlapping rs17594362) and Rgcc-E2 (overlapping rs12429256), respectively. The other seven putative OL enhancers either lack H3K27ac signals in the brain tissues or are associated with weak non-specific H3K27ac signals (Fig. S1), and we did not pursue them further. Of note, there is no spinal cord H3K27ac ChIP-seq data in the Roadmap Epigenomics Project.

To corroborate the conclusion that Rgcc-E1 and Rgcc-E2 are OL enhancers, we performed a luciferase assay. To this end, we cloned Rgcc-E1 and Rgcc-E2 into pGL3-promoter (see **Materials and Methods**), and they were transfected into primary OPCs purified from mouse pups by immunopanning (18, 19). Our previous study has shown that luciferase reporter constructs transfected into primary OPCs persist in them at least for 3 days in culture (20). For a potential condition-dependent enhancer activity of Rgcc-E1 and Rgcc-E2, transfected OPCs were split into two and cultured in the proliferation and differentiation conditions, respectively. Our culture conditions were as described by Emery and Dugas (18). The proliferation and differentiation of mouse OPCs in these culture conditions were validated by marker expression (Fig. S2) and also monitored by Rffl, a specific and sensitive Myrf luciferase reporter (20–22), which was generated by cloning a Myrf ChIP-seq peak (rn4 chr10:71034166–71 034 749) into pGL3-promoter. Since Myrf is expressed in differentiating OLs, but not in OPCs (23, 24), the reporter activity of Rffl increases upon the differentiation of OPCs. Compared to pGL3-promoter (the empty vector control), Rgcc-E1 and Rgcc-E2 significantly activated transcription in both the proliferation and differentiation conditions (*P value $< 2.0 \times 10^{-3}$ by one sample two-sided Student's *t* test corrected by the Bonferroni procedure, Fig. 2A), demonstrating that Rgcc-E1 and Rgcc-E2 work as enhancers in OL lineage cells. The increased activity of Rffl in the differentiation condition compared to the proliferation condition is indicative of the differentiation of transfected OPCs in the differentiation condition. Given the two-fold increase in the reporter activity of Rffl, we estimate that transfected OPCs cultured in the differentiation condition were still in their early stage of differentiation.

We also examined the OL ChIP-seq data underlying Rgcc-E1 and Rgcc-E2 (Fig. 2B). The OL H3K27ac ChIP-seq data revealed a pronounced peak-valley-peak pattern for Rgcc-E1 (25), indicative of its enhancer activity. The peak-valley-peak pattern was also there for Rgcc-E2, but much weaker. In stark contrast, there was no peak whatsoever for Rgcc-E1 and Rgcc-E2 in the H3K4me3 ChIP-seq data (25), in keeping with their enhancer identity. Brg1 and Chd7, two important OL epigenetic regulators (25–27), bound to Rgcc-E1 and Rgcc-E2, suggesting that they may be involved in the epigenetic activation of Rgcc-E1 and Rgcc-E2. Olig2, Sox10 and Tcf7l2 play a critical role in OL development (25, 28–31), and they all bound to Rgcc-E1 and Rgcc-E2. Notably, Sox10 bound to Rgcc-E1 and Rgcc-E2 in the mouse spinal cord (31), signifying *in vivo* enhancer activity, which is consistent with the brain tissue H3K27ac ChIP-seq data from the Roadmap Epigenomics Project. Collectively, we conclude that Rgcc-E1 and Rgcc-E2 are bona fide OL enhancers that are conserved between human, mouse and rat.
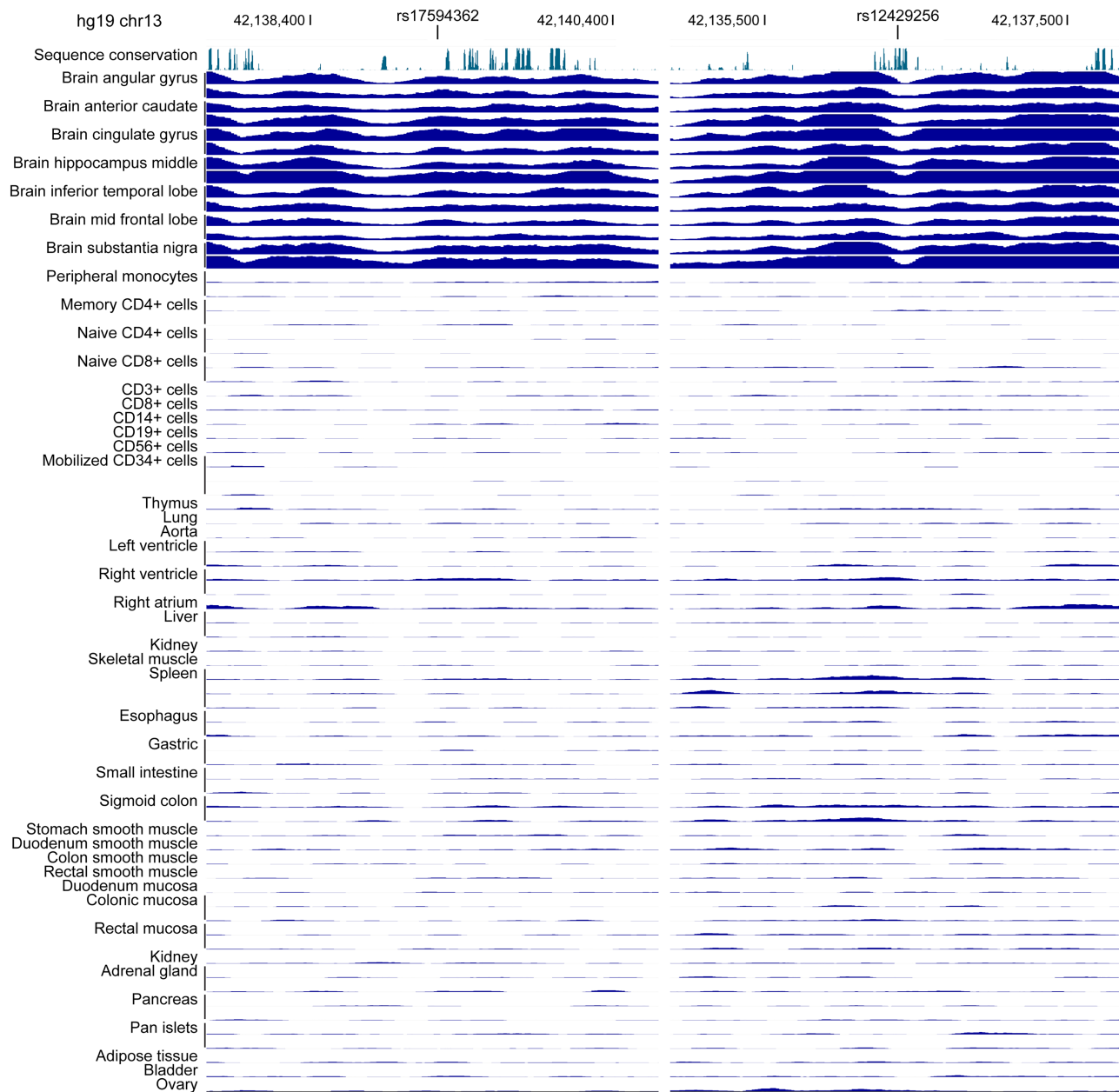
Figure 1. The NIH Roadmap Epigenomics Project H3K27ac ChIP-seq data for rs17594362 and rs12429256. These H3K27ac ChIP-seq data were visualized by the WASHU Epigenome Browser.

The risk alleles of rs17594362 and rs12429256 up-regulate the enhancer activity of Rgcc-E1 and Rgcc-E2

Having confirmed that Rgcc-E1 and Rgcc-E2 are OL enhancers, we set out to determine how the risk alleles of rs17594362 and rs12429256 affect the enhancer activity of Rgcc-E1 and Rgcc-E2. By site-directed mutagenesis, we introduced the risk alleles to Rgcc-E1 and Rgcc-E2 in pGL3-promoter (T for Rgcc-E1 and A for Rgcc-E2), generating Rgcc-E1^T and Rgcc-E2^A. By a luciferase assay, we compared their enhancer activity with that of their protective counterparts, Rgcc-E1^C and Rgcc-E2^C. Rgcc-E1^T, Rgcc-E1^C, Rgcc-E2^A and Rgcc-E2^C were transfected into primary mouse OPCs, and transfected OPCs cultured in the proliferation and differentiation conditions, as above. We found that the risk

alleles of rs17594362 and rs12429256 significantly up-regulate the enhancer activity of Rgcc-E1 and Rgcc-E2 in both the proliferation and differentiation conditions ($^*P < 3.5 \times 10^{-2}$ by unpaired two-sided Student's *t* test corrected by the Bonferroni procedure, Fig. 2C). These observations indicate that the risk alleles of rs17594362 and rs12429256 render Rgcc-E1 and Rgcc-E2 hyperactive throughout the OL lineage.

Chromatin interaction data suggest that Rgcc is the primary target of Rgcc-E1 and Rgcc-E2

In order to decode the functional mechanism of rs17594362 and rs12429256, it is necessary to identify the target gene of
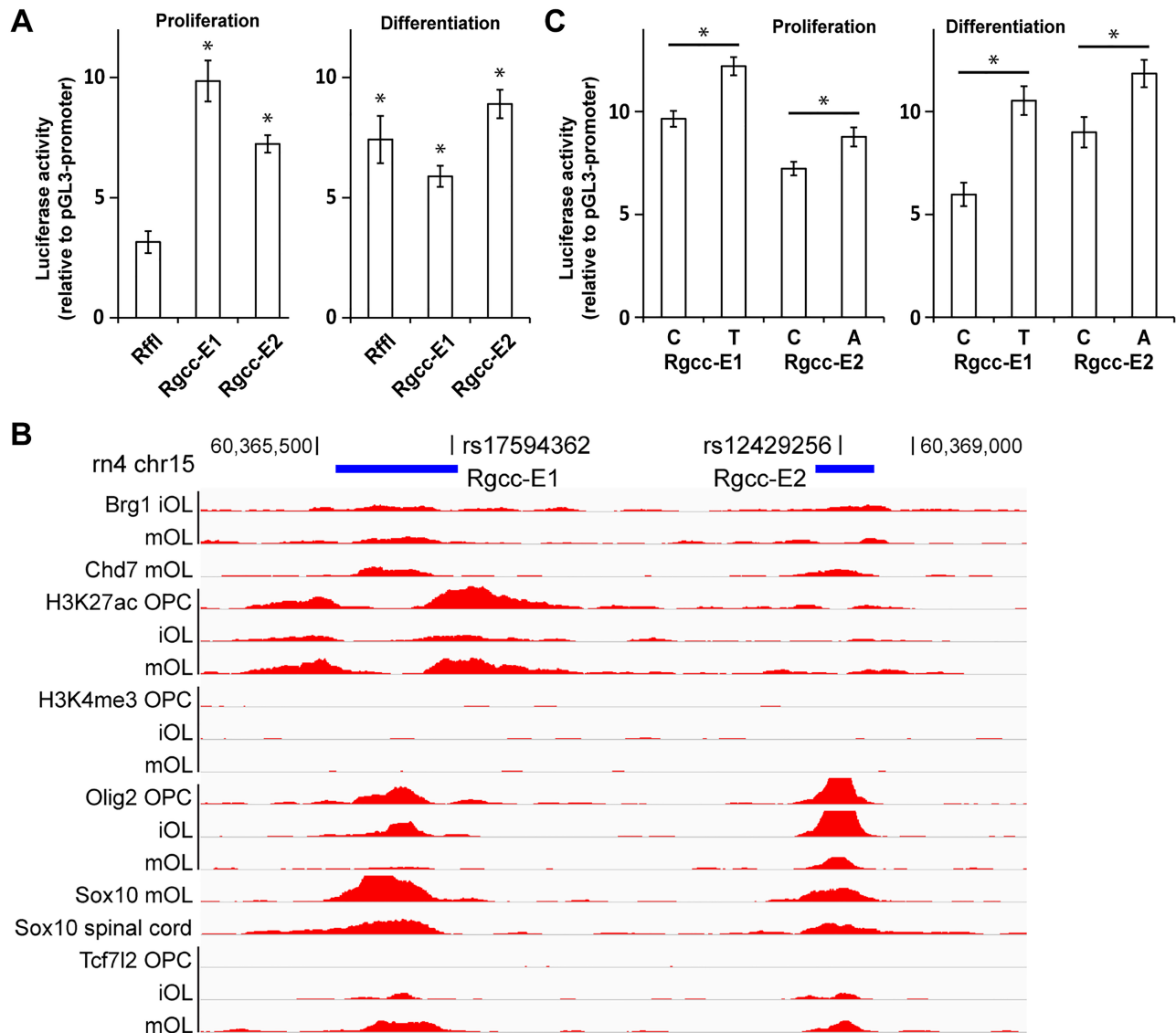
Figure 2. The enhancer activity of Rgcc-E1 and Rgcc-E2 in OL lineage cells and the effect of rs17594362 and rs12429256. (**A**) The enhancer activity of Rgcc-E1 and Rgcc-E2 cloned in pGL3-promoter was compared with that of pGL3-promoter (the empty vector) in primary mouse OPCs cultured in the proliferating and differentiating conditions. Shown are the means and standard errors ($n = 8$). *P value $< 2.0 \times 10^{-3}$ by one sample two-sided Student's t test corrected by the Bonferroni procedure. (**B**) The rat OL ChIP-seq data underlying Rgcc-E1 and Rgcc-E2. (**C**) The effect of rs17594362 and rs12429256 on the enhancer activity of Rgcc-E1 and Rgcc-E2 in primary mouse OPCs cultured in proliferating and differentiating conditions. Shown are the means and standard errors ($n = 8$). *P $< 3.5 \times 10^{-2}$ by unpaired two-sided Student's t test corrected by the Bonferroni procedure.

Rgcc-E1 and Rgcc-E2. To this end, we examined public chromatin interaction data to find a topologically associating domain (TAD) where Rgcc-E1 and Rgcc-E2 belong. An eye-opening discovery from chromatin conformation capture studies is that a gene and its enhancer tend to be found in the same TAD (32, 33), a fundamental unit of genome organization and function (34–37). Hence, the TAD information would allow us to make an educated guess about the target gene of Rgcc-E1 and Rgcc-E2, two closely spaced OL enhancers. There are two features of a TAD that need to be distinguished—internal detail and boundaries. The internal detail of a TAD reflects cell type-specific interactions among genes and enhancers, and it differs between cell types. In contrast, the boundaries of a TAD tend to be conserved between cell types and species (32). Thus, even if there is no chromatin interaction data for OL lineage cells, we can still delineate the

TAD for Rgcc-E1 and Rgcc-E2 by analyzing public chromatin interaction data for other cell types. We have successfully used this approach in our recent study for OL enhancers governing Myrf expression (14).

In order to delineate the TAD where Rgcc-E1 and Rgcc-E2 belong, we analyzed kilobase-resolution Hi-C data for seven diverse cell types from human and mouse (33). The TAD organization around Rgcc-E1 and Rgcc-E2 is well defined and conserved between cell types and species (demarcated in green for IMR90 and CH12-LX, Fig. 3A). Please note that Rgcc-E1 and Rgcc-E2 are very close to each other (just 3 Kb apart on chromosome 13). In Figure 3A, they look like a single spot, whose location is marked by thin black crossing lines. The syntenic region that encompasses Rgcc and the two OL enhancers is flipped in mouse compared to human. Notably, this flip is also mirrored in the
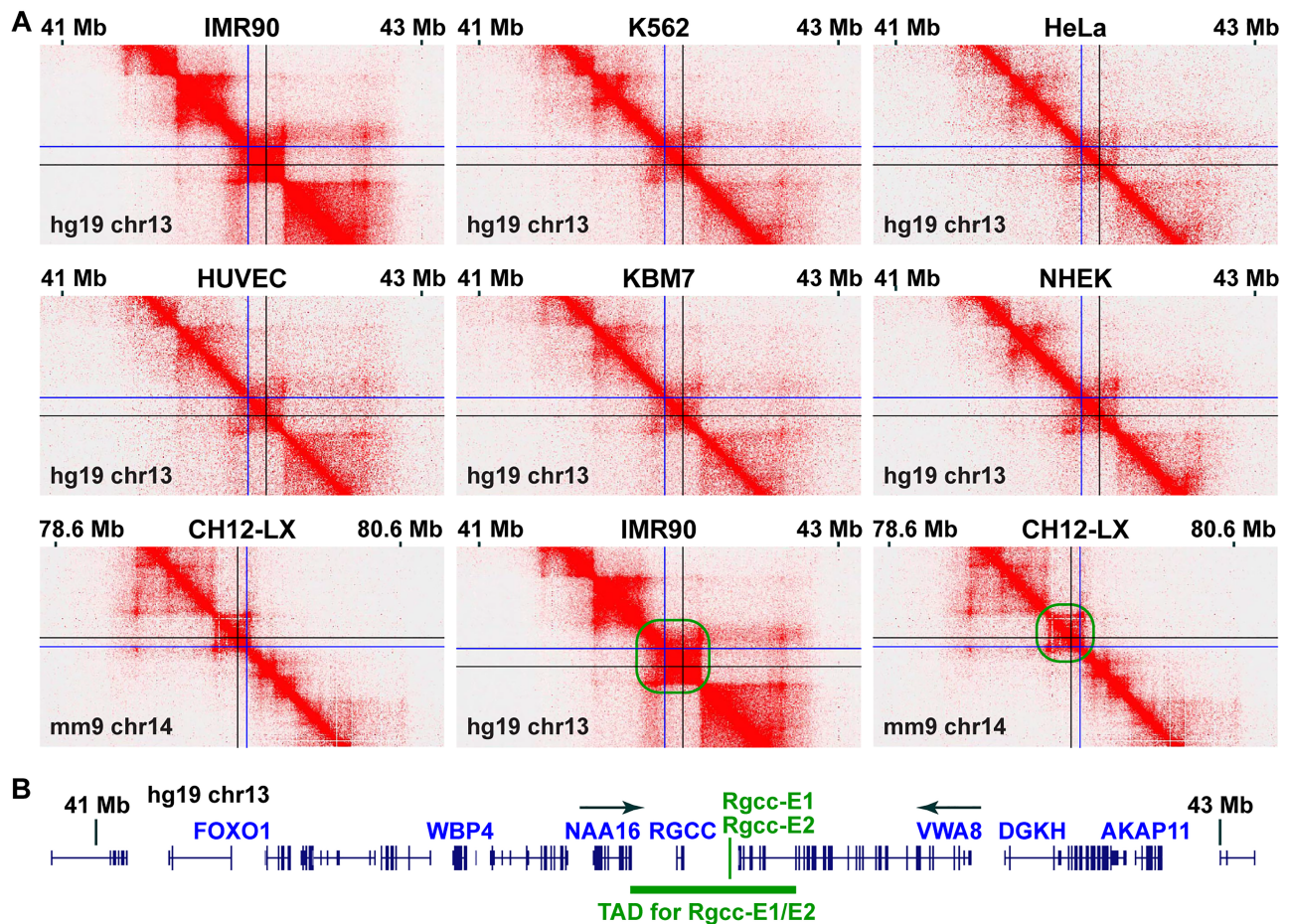
Figure 3. Chromatin interaction data suggest that Rgcc is the primary target of Rgcc-E1 and Rgcc-E2. (**A**) The publicly available 5 Kb-resolution Hi-C data for 7 diverse cell types from human and mouse were analyzed to delineate the TAD for Rgcc-E1 and Rgcc-E2 (33). The interaction frequency between two loci is indicated by color: white means no interaction, and red the strongest possible interaction. The position of Rgcc-E1 and Rgcc-E2 is marked by thin black crossing lines. The position of Rgcc is marked by thin blue crossing lines. The Rgcc-E1/E2 TAD is demarcated in green for IMR90 and CH12-LX. IMR90: lung fibroblast. K562 and KBM7: chronic myelogenous leukemia cells. HeLa: cervical cancer cell. HUVEC: human umbilical vein endothelial cell. NHEK: normal human epidermal keratinocyte. CH12-LX: murine CH12 B-cell lymphoma cell. (**B**) The TAD for Rgcc-E1 and Rgcc-E2 contains one protein-coding gene, Rgcc. Naa16 and Vwa8 are its neighbors, but their promoters are found out of the TAD.
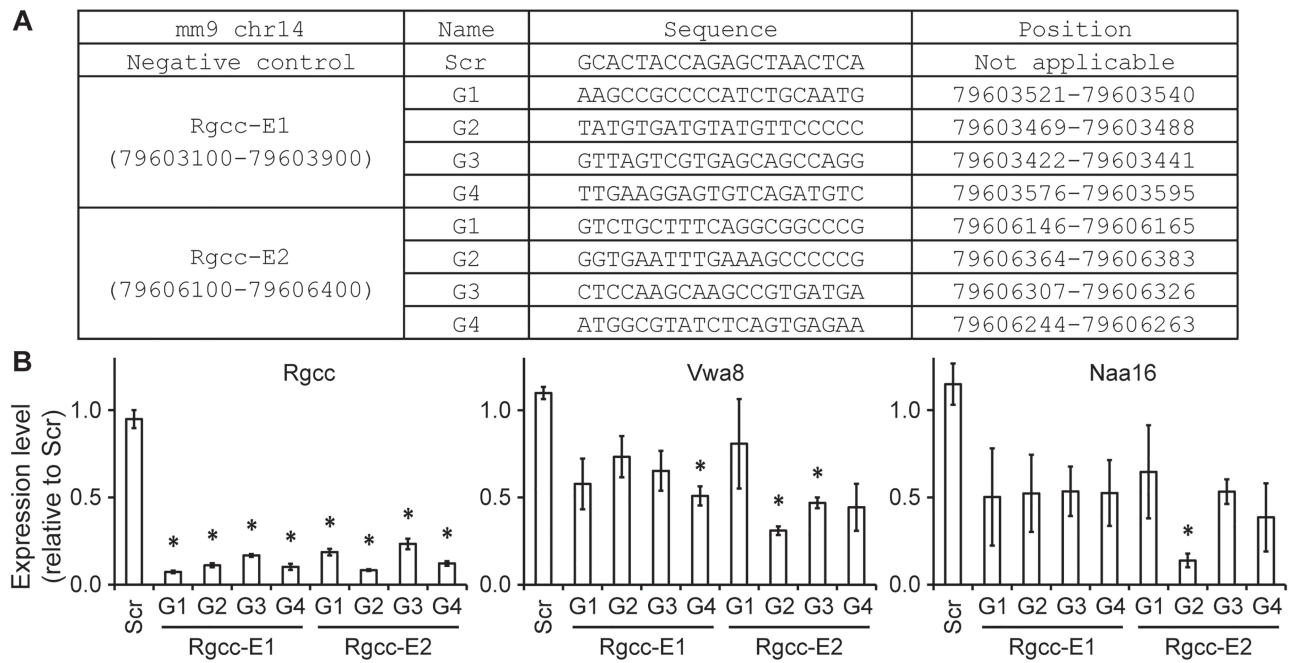
TAD organization (CH12-LX, Fig. 3A), highlighting a high degree conservation of the TAD organization in this region through evolution. The Rgcc-E1 and Rgcc-E2 TAD spans about 350 Kb in the human genome (Fig. 3B). Remarkably, there is only one protein-coding gene in this TAD, which is Rgcc (its promoter location is marked by thin blue crossing lines in Fig. 3A). This immediately suggests that Rgcc is the primary target of Rgcc-E1 and Rgcc-E2. Vwa8 and Naa16 are close to this TAD, but their promoters are found outside of the TAD (arrows in Fig. 3B), suggesting that they are unlikely to be the primary target of Rgcc-E1 and Rgcc-E2.

Epigenome editing confirms that Rgcc is the primary target of Rgcc-E1 and Rgcc-E2

To find whether Rgcc is a target gene of Rgcc-E1 and Rgcc-E2, we performed epigenome editing experiments using CRISPRi (CRISPR interference), a cutting-edge epigenome editing technique (38–42). In CRISPRi, dCas9-KRAB, a fusion protein between a nuclease-null Cas9 (dCas9) and a KRAB (Krüppel associated box) domain, is targeted to a specific locus by guide

RNAs (gRNAs). When targeted to the promoter of a gene, dCas9-KRAB inactivates it, decreasing gene expression (38, 39). When targeted to an enhancer, dCas9-KRAB silences it, subsequently down-regulating its target genes (40–43). This is how CRISPRi allows one to find target genes of a given enhancer.

To deliver dCas9-KRAB to Rgcc-E1 and Rgcc-E2, we designed four gRNAs for each enhancer (designated as G1 through G4, Fig. 4A). For stable and inducible CRISPRi, we generated nine Oli-neu cell lines. Oli-neu cells are a widely used mouse OL cell line (44). One cell line stably expresses Scr, a non-targeting negative control gRNA (Fig. 4A). Four cell lines stably express the four gRNAs for Rgcc-E1. The other four lines stably express the four gRNAs for Rgcc-E2. These nine Oli-neu cell lines also express dCas9-KRAB in a doxycycline-dependent manner. To execute CRISPRi, doxycycline was added to the culture media for 2 days before RNA harvest. RT-qPCR analysis showed that when dCas9-KRAB is targeted to Rgcc-E1 by any of the four gRNAs, Rgcc expression goes down by more than 80% (*$P < 4.7 \times 10^{-4}$ by unpaired two-sided Student's t test corrected by the Bonferroni procedure, Fig. 4B). Rgcc expression decreased similarly when dCas9-KRAB was targeted to Rgcc-E2 (*$P < 1.2 \times 10^{-3}$ by unpaired two-sided Student's t test corrected by the Bonferroni procedure,

A

mm9 chr14	Name	Sequence	Position
Negative control	Scr	GCACTACCAGAGCTAACTCA	Not applicable
Rgcc-E1 (79603100–79603900)	G1	AAGCCGCCCCATCTGCAATG	79603521–79603540
	G2	TATGTGATGTATGTTCCCCC	79603469–79603488
	G3	GTTAGTCGTGAGCAGCCAGG	79603422–79603441
	G4	TTGAAGGAGTGTCAGATGTC	79603576–79603595
Rgcc-E2 (79606100–79606400)	G1	GTCTGCTTTCAGGCGGCCCG	79606146–79606165
	G2	GGTGAATTTGAAAGCCCCCG	79606364–79606383
	G3	CTCCAAGCAAGCCGTGATGA	79606307–79606326
	G4	ATGGCGTATCTCAGTGAGAA	79606244–79606263

B

Figure 4. Epigenome editing shows that Rgcc is the primary target of Rgcc-E1 and Rgcc-E2. (**A**) gRNAs used for epigenome editing experiments. Scr is a non-targeting negative control gRNA. For each of Rgcc-E1 and Rgcc-E2, four gRNAs were designed. (**B**) Rgcc-E1 and Rgcc-E2 were silenced by dCas9-KRAB in Oli-neu cells, and its effect on the expression of Rgcc, Vwa8 and Naa16 determined by RT-qPCR. Shown are the means and standard errors ($n = 3$). For Rgcc and Rgcc-E1, $*P < 4.7 \times 10^{-4}$. For Rgcc and Rgcc-E2, $*P < 1.2 \times 10^{-3}$. For Vwa8 and Rgcc-E1, $*P < 3.3 \times 10^{-3}$. For Vwa8 and Rgcc-E2, $*P < 7.0 \times 10^{-4}$. For Naa16 and Rgcc-E2, $*P < 5.1 \times 10^{-3}$. All P values by unpaired two-sided Student's t test corrected by the Bonferroni procedure.

Fig. 4B). Since the same results were obtained for Rgcc-E1 and Rgcc-E2 with multiple independent gRNAs, we conclude that Rgcc is a target gene of Rgcc-E1 and Rgcc-E2, ruling out the off-target effects of CRISPRi. It is interesting to note that although Rgcc-E1 and Rgcc-E2 are about 100 Kb apart from the Rgcc promoter, they have a powerful influence on Rgcc expression.

Having found that Rgcc is a target gene of Rgcc-E1 and Rgcc-E2, we asked whether Rgcc is their primary target. To this end, the same RNA samples were analyzed for Vwa8 and Naa16, two neighboring genes of Rgcc (Fig. 3B). Silencing Rgcc-E1 by dCas9-KRAB did not have a significant effect on the expression of Vwa8 and Naa16 (Fig. 4B); only G4 reached statistical significance for Vwa8. Two-way analysis of variance (ANOVA) confirmed the differential effect of Rgcc-E1 on Rgcc versus Vwa8 and Naa16 (P value corrected by the Bonferroni procedure $< 9.1 \times 10^{-3}$). These results indicate that Rgcc is the primary target of Rgcc-E1. Similarly, knockdown of Rgcc-E2 by dCas9-KRAB had a much weaker effect on Vwa8 and Naa16 than on Rgcc (two-way ANOVA P value corrected by the Bonferroni procedure $< 3.3 \times 10^{-2}$). Taken together, Rgcc is the primary target of Rgcc-E1 and Rgcc-E2. Of note, there is an overall downward trend for Vwa8 and Naa16 when Rgcc-E1 and Rgcc-E2 are silenced by dCas9-KRAB. This suggests that the boundaries of the TAD that contains Rgcc-E1 and Rgcc-E2 do not insulate these enhancers perfectly and that Rgcc-E1 and Rgcc-E2 have a secondary weak effect on Vwa8 and Naa16 (45).

Expression quantitative trait loci analysis confirms the molecular mechanism of rs17594362 and rs12429256

Our data so far suggest that rs17594362 and rs12429256 induce Rgcc overexpression by potentiating the enhancer activity of Rgcc-E1 and Rgcc-E2. To gain further support for this molecular mechanism, we examined eQTL data from the GTEx project (15). Simply speaking, an expression quantitative trait locus is a locus whose allele is significantly correlated with the expression level of a gene. By correlating gene expression with common SNPs, the GTEx project has identified eQTL for many genes in various human tissues and cell lines. If our molecular mechanism were correct, rs17594362 and rs12429256 might show up as eQTL for Rgcc in some tissues or cell lines. Indeed, the GTEx eQTL data show that rs17594362 and rs12429256 are Rgcc eQTL in several tissues and cell lines (Table 1). There are two important points to note about these eQTL data. First, the effect size of rs17594362 and rs12429256 for Rgcc is always positive (Table 1), meaning that the dosage of the risk allele is always positively correlated with Rgcc expression level. It confirms our molecular mechanism that the two MS SNPs act by inducing Rgcc overexpression. Second, Rgcc is the one and only gene for which rs17594362 and rs12429256 are eQTL, meaning that any effect on gene expression that arises from the two MS SNPs is specifically targeted to Rgcc. It is consistent with our epigenome editing results showing that Rgcc is the primary target of Rgcc-E1 (rs17594362) and Rgcc-E2 (rs12429256). Of note, rs17594362 and rs12429256 did not come out as Rgcc eQTL in the brain and spinal cord, most likely because many cell type-specific signals are lost in complex tissue samples (46). On the other hand, the observation that rs17594362 and rs12429256 are Rgcc eQTL in tissues that do not contain OL lineage cells suggests that Rgcc-E1 and Rgcc-E2 are also active in other cell types.

Discussion

MS is commonly known as an autoimmune demyelinating disease of the central nervous system. However, its cause remains elusive. To gain insight into the etiology of MS, the

Table 1. The GTEx eQTL data for rs17594362 and rs12429256

SNP	Gene	Tissue	# of samples	Effect size	P value
rs17594362 (Rgcc-E1)	Rgcc	Adipose—subcutaneous	385	0.58	$4.20E^{-12}$
		Muscle—skeletal	491	0.35	$3.00E^{-07}$
		Nerve—tibial	361	0.33	$9.70E^{-19}$
		Esophagus—muscularis	335	0.29	$2.20E^{-06}$
		Skin—sun exposed (lower leg)	414	0.24	$1.10E^{-06}$
		Cells—transformed fibroblasts	300	0.19	$9.20E^{-06}$
rs12429256 (Rgcc-E2)	Rgcc	Adipose—subcutaneous	385	0.46	$1.20E^{-08}$
		Muscle—skeletal	491	0.34	$1.50E^{-07}$
		Nerve—tibial	361	0.31	$7.20E^{-19}$
		Esophagus—muscularis	335	0.30	$6.10E^{-07}$
		Skin—sun exposed (lower leg)	414	0.22	$3.10E^{-06}$

These data were downloaded from the GTEx project website. Only eQTL with $P < 1.0 \times 10^{-5}$ are shown.

International MS Genetics Consortium has conducted a large-scale GWAS, identifying 102 SNPs for MS susceptibility (9). The SNP rs17594362 is among the 102 MS SNPs. Our study shows that rs17594362 and rs12429256, a SNP in linkage disequilibrium with rs17594362 ($r^2 = 1$), up-regulate Rgcc-E1 and Rgcc-E2, respectively. Chromatin interaction data and epigenome editing experiments indicate that Rgcc is the primary target of Rgcc-E1 and Rgcc-E2. Taken together, our study finds that rs17594362 and rs1229256 up-regulate the expression of Rgcc by potentiating the enhancer activity of Rgcc-E1 and Rgcc-E2. Importantly, this molecular mechanism is well supported by the eQTL data of the GTEx project (15).

A remaining issue for the molecular mechanism of rs17594362 and rs1229256 is how they up-regulate the enhancer activity of Rgcc-E1 and Rgcc-E2. For the rs17594362/Rgcc-E1 case, our computational analysis suggests that Sox family transcription factors may play a role. The protective allele of rs17594362 is C, and the DNA sequence around it is CCCTTGT, where the underlined C is the protective allele. For the risk allele T, the sequence is changed to CCTTTGT, which is a better match to the Sox motif than CCCTTGT. Sox family transcription factors may preferentially bind to the risk allele, potentiating the enhancer activity of Rgcc-E1. On the other hand, Ets family transcription factors may be responsible for the rs12429256/Rgcc-E2 case. The protective allele of rs12429256 is C, and the DNA sequence around it is GGCA, where the underlined C is the protective allele. For the risk allele A, the sequence is changed to GGAA, which is a better match to the Ets motif than GGCA. Ets family transcription factors may keep Rgcc-E2 hyperactive in the presence of the risk allele, inducing Rgcc overexpression.

While our study has elucidated the molecular mechanism of rs17594362 and rs12429256, it does not address their cellular mechanism, which is beyond the scope of the current study. To address the cellular mechanism of the two MS SNPs, one first has to elucidate in which cell type rs17594362 and rs12429256 up-regulate Rgcc expression. Our study and the NIH Roadmap Epigenomics Project data suggest, but do not prove, that OL lineage cells are one such cell type. At present, there is no solid evidence directly proving that rs17594362 and rs12429256 up-regulate Rgcc expression in OL lineage cells. This is why the current study did not address the impact of Rgcc overexpression on OL differentiation. If rs17594362 and rs12429256 indeed increase the expression level of Rgcc in OL lineage cells, we expect it to negatively impact OL development for the following reason. Rgcc is a multifunctional molecule with a prominent role in cell cycle activation (47–50). Not much is known about its role in OL lineage cells except that it enhances the proliferation of OPCs *in vitro* (47, 50). Consistent with its role in cell proliferation, it is highly expressed in OPCs, but not in differentiating OLs (51). Given this expression profile, Rgcc overexpression in OL lineage cells may interfere with their proper differentiation in two different ways that are not mutually exclusive. First, given that Rgcc activates the proliferation of OPCs *in vitro*, Rgcc overexpression may indirectly inhibit their differentiation by tipping the balance of proliferation versus differentiation toward proliferation, since proliferation and differentiation are mutually exclusive for OPCs (52, 53). Second, in light of its pleiotropic role in signal transduction and the pathological activation of fibroblasts and astrocytes (49, 54, 55), Rgcc overexpression may directly impair the differentiation process. Further, if Rgcc, which is barely expressed in mature OLs (51), continues to be expressed in mature OLs, their differentiated state may be perturbed.

Another important issue regarding the cellular mechanism of rs17594362 and rs12429256 is whether there are any other cell types than OL lineage cells where rs17594362 and rs12429256 up-regulate Rgcc expression. The NIH Roadmap Epigenomics Project data show that Rgcc-E1 and Rgcc-E2 are highly specific to the central nervous system (CNS). Although the eQTL data of the GTEx project indicate that rs17594362 and rs12429256 increase Rgcc expression in cell types outside of the CNS, those cell types must be rare in light of the Roadmap Epigenomics Project H3K27ac ChIP-seq data (Fig. 1). Consistently, a recent single-cell ATAC-seq study from the Shendure laboratory shows that Rgcc-E1 and Rgcc-E2 are primarily active in OL lineage cells and astrocytes (46). Collectively, rs17594362 and rs12429256 are likely to confer genetic risk for MS by increasing Rgcc expression in OL lineage cells and/or astrocytes. Notably, the single-cell ATAC-seq data indicate that Rgcc-E1 and Rgcc-E2 are not active in immune cells, which is in line with the Roadmap Epigenomics Project H3K27ac ChIP-seq data (Fig. 1). Hence, while the Rgcc gene itself is expressed in diverse cell types, including immune cells, Rgcc-E1 (associated with rs17594362) and Rgcc-E2 (associated with rs12429256) are specific to OL lineage cells and astrocytes, which is why rs17594362 and rs12429256 are not expected to work through immune cells. Our future study will determine whether rs17594362 and rs12429256 up-regulate Rgcc expression in OL lineage cells and astrocytes. Once we identify the cell type in which rs17594362 and rs12429256 exert their effects, we will elucidate the cellular effect of Rgcc overexpression, shedding light on how the two MS SNPs increase the risk of MS.

Materials and Methods

Constructs and cell lines Rgcc-E1 (hg19 chr13:42139139–42 139 932) and Rgcc-E2 (hg19 chr13:42136177–42 136 600) were cloned into pGL3-promoter (Promega). Human genomic DNA was purchased from Promega (#G1471), and Rgcc-E1 and Rgcc-E2 amplified from it by PCR. Site-directed mutagenesis was performed by a PCR-based method to introduce the risk alleles of rs17594362 and rs12429256 into Rgcc-E1 and Rgcc-E2, respectively. To generate an inducible dCas9-KRAB construct, a dTomato-P2A-blasticidin cassette was amplified from pSBbi-RB (Addgene #60522) by PCR and inserted into pAAVS1-NDi-CRISPRi (Addgene #73497). This plasmid was inserted into the Rosa26 locus of Oli-neu cells (44) by CRISPR/Cas9, and correctly modified cells were selected by blasticidin resistance and dTomato expression. These cells express dCas9-KRAB in a doxycycline-dependent manner. To generate gRNA expression vectors, the EF-1α promoter of pSBbi-GP (Addgene #60511) was replaced by the gRNA scaffold taken from lentiCRISPR v2 (Addgene #52961). Guide RNAs were designed by using a web service from the Zhang laboratory (zlab.bio/guide-design-resources). The gRNA plasmid was inserted into the genome of the dCas9-KRAB Oli-neu cell line by SB100X (56), a hypersensitive transposon. The sequence information of all constructs was verified by Sanger sequencing.

Animal procedures, tissue harvest and cell culture The current study was conducted in strict accordance with the protocol approved by the Institutional Animal Care and Use Committee of SUNY Buffalo (protocol #NA-Park2). OPCs were purified from mouse pups of P7 $\sim$ P9 by immunopanning (19). The original immunopanning protocol for mouse OPCs (18) did not work well in our hands. Instead, we found that the immunopanning protocol for rat OPCs works well for mouse OPCs, and this is why we used it to purify mouse OPCs. Primary mouse OPCs and Oli-neu cells were kept in a proliferative condition by supplementing the Sato media (19) with PDGF (10 µg/mL), NT3 (1 µg/mL), CNTF (10 µg/mL) and NeuroCult™ SM1 Neuronal Supplement. Both were maintained in a humidified 8% CO_2 incubator at 37°C. Transient transfection was performed using Lipofectamine 2000 as per the manufacturer's instructions.

Computational analysis The NIH Roadmap Epigenomics Project data were visualized by the WASHU Epigenome Browser (http://epigenomegateway.wustl.edu/legacy). The OL ChIP-seq data were downloaded from the Sequence Read Archive. Their accession numbers are as follows: Brg1 (GSM1040154, GSM1040155), Chd7 (GSM1869162), H3K27ac (GSM1040159, GSM1040160, GSM1040161), H3K4me3 (GSM1040162, GSM1040163, GSM1040164), Olig2 (GSM1040156, GSM1040157, GSM1040158), Sox10 (GSM1869163, GSM1577133, GSM1577134), Tcf7l2 (GSM1587566, GSM1587567, GSM1587568). Hi-C data were visualized by Juicebox (57). Expression quantitative trait loci data were downloaded from the GTEx website (https://www.gtexportal.org/home/index.html). The single-cell mouse ATAC-seq data (46) were downloaded from the Shendure laboratory website (http://atlas.gs.washington.edu/mouse-atac). Genomic coordinates were mapped among hg38, hg19, mm9 and rn4 by the LiftOver function of the UCSC Genome Browser.

Luciferase assay Luciferase assays were performed using the dual luciferase reporter assay kit (Promega) as per the manufacturer's instructions. Primary mouse OPCs were transfected with pRL-TK (an internal control) and pGL3-promoter/Rgcc-E1/Rgcc-E2. Firefly and Renilla luciferase activities were measured, and their ratios calculated to estimate enhancer activity.

Table 2. Primer sequences for RT-qPCR

Rgcc	F	GGCTTCAGCGACTCGGAG
	R	CTTTCCGAGGAGTGACAGCG
Vwa8	F	CTCATGTCTGCGGAGCGC
	R	GTACCTGGGCACTGGCAAG
Naa16	F	GGGTGTCCACCTCTGTTCACTAC
	R	CTTCTCCCCGTTCTCATAAGGGC
Gapdh	F	GGTGAAGGTCGGTGTGAACGG
	R	CTGGAACATGTAGACCATGTAGTTGAGG

RT-qPCR Total RNA was purified using Trizol (Thermo Fisher Scientific #15596026), and cDNA synthesized by the SuperScript First-Strand kit (Invitrogen #11904-018). Quantitative PCR was performed by C1000 Touch thermal cycler with the CFX384 optical reaction module (Bio-rad) to quantify the mRNA expression levels of Rgcc, Vwa8, Naa16 and Gapdh. The expression level of a gene was normalized by that of Gapdh. Each PCR reaction contained 2 µL of cDNA, 5 µL of the iTaq Universal SYBR Green Supermix (Bio-rad #1725124) and 500 nM of forward and reverse primers. The primer sequences are shown in Table 2.

Supplementary Material

Supplementary Material is available at *HMG* online.

References

1. Trapp, B.D. and Nave, K.-A. (2008) Multiple sclerosis: an immune or neurodegenerative disorder? *Annu. Rev. Neurosci.*, **31**, 247–269.
2. Hauser, S.L., Chan, J.R. and Oksenberg, J.R. (2013) Multiple sclerosis: prospects and promise. *Ann. Neurol.*, **74**, 317–327.
3. Dendrou, C.A., Fugger, L. and Friese, M.A. (2015) Immunopathology of multiple sclerosis. *Nat. Rev. Immunol.*, **15**, 545–558.
4. Nakahara, J., Maeda, M., Aiso, S. and Suzuki, N. (2012) Current concepts in multiple sclerosis: autoimmunity versus oligodendrogliopathy. *Clin. Rev. Allergy Immunol.*, **42**, 26–34.
5. Stys, P.K., Zamponi, G.W., van Minnen, J. and Geurts, J.J.G. (2012) Will the real multiple sclerosis please stand up? *Nat. Rev. Neurosci.*, **13**, 507–514.
6. Ip, C.W., Kroner, A., Bendszus, M., Leder, C., Kobsar, I., Fischer, S., Wiendl, H., Nave, K.-A. and Martini, R. (2006) Immune cells contribute to myelin degeneration and axonopathic changes in mice overexpressing proteolipid protein in oligodendrocytes. *J. Neurosci.*, **26**, 8206–8216.
7. Caprariello, A.V., Mangla, S., Miller, R.H. and Selkirk, S.M. (2012) Apoptosis of oligodendrocytes in the central nervous system results in rapid focal demyelination. *Ann. Neurol.*, **72**, 395–405.

8. Traka, M., Podojil, J.R., McCarthy, D.P., Miller, S.D. and Popko, B. (2015) Oligodendrocyte death results in immune-mediated CNS demyelination. *Nat. Neurosci.*, **19**, 65–74.

9. The International Multiple Sclerosis Genetics Consortium (2011) Genetic risk and a primary role for cell-mediated immune mechanisms in multiple sclerosis. *Nature*, **476**, 214–219.

10. Mika, K.M., Li, X., DeMayo, F.J. and Lynch, V.J. (2018) An ancient fecundability-associated polymorphism creates a GATA2 binding site in a distal enhancer of HLA-F. *Am. J. Hum. Genet.*, **103**, 509–521.

11. Peserico, A., Loconte, D.C., Susca, F.C., Resta, N., Sanese, P., Bagnulo, R., Lovaglio, R., Tezil, T., Grossi, V., Simone, C. et al. (2018) The longevity SNP rs2802292 uncovered: HSF1 activates stress-dependent expression of FOXO3 through an intronic enhancer. *Nucleic Acids Res.*, **46**, 5587–5600.

12. Kycia, I., Wolford, B.N., Huyghe, J.R., Fuchsberger, C., Vadlamudi, S., Kursawe, R., Welch, R.P., Albanus, R.D.O., Uyar, A., Khetan, S. et al. (2018) A common type 2 diabetes risk variant potentiates activity of an evolutionarily conserved islet stretch enhancer and increases C2CD4A and C2CD4B expression. *Am. J. Hum. Genet.*, **102**, 620–635.

13. Chen, X.-F., Zhu, D.-L., Yang, M., Hu, W.-X., Duan, Y.-Y., Lu, B.-J., Rong, Y., Dong, S.-S., Hao, R.-H., Chen, J.-B. et al. (2018) An osteoporosis risk SNP at 1p36.12 acts as an allele-specific enhancer to modulate LINC00339 expression via long-range loop formation. *Am. J. Hum. Genet.*, **102**, 776–793.

14. Kim, D., An, H., Shearer, R.S., Sharif, M., Fan, C., Choi, J.-o., Ryu, S. and Park, Y. (2019) A principled strategy for mapping enhancers to genes. *Sci. Rep.*, **9**, 11043.

15. Lonsdale, J., Thomas, J., Salvatore, M., Phillips, R., Lo, E., Shad, S., Hasz, R., Walters, G., Garcia, F., Young, N. et al. (2013) The genotype-tissue expression (GTEx) project. *Nature Genet.*, **45**, 580–585.

16. The Roadmap Epigenomics Consortium (2015) Integrative analysis of 111 reference human epigenomes. *Nature*, **518**, 317–330.

17. Creyghton, M.P., Cheng, A.W., Welstead, G.G., Kooistra, T., Carey, B.W., Steine, E.J., Hanna, J., Lodato, M.A., Frampton, G.M., Sharp, P.A. et al. (2010) Histone H3K27ac separates active from poised enhancers and predicts developmental state. *Proc. Natl. Acad. Sci. USA*, **107**, 21931–21936.

18. Emery, B. and Dugas, J.C. (2013) Purification of oligodendrocyte lineage cells from mouse cortices by immunopanning. *Cold Spring Harb. Protoc.*, **2013**, 854–868.

19. Dugas, J.C. and Emery, B. (2013) Purification of oligodendrocyte precursor cells from rat cortices by immunopanning. *Cold Spring Harb. Protoc.*, **2013**, 745–758.

20. Kim, D., Choi, J.-o., Fan, C., Shearer, R.S., Sharif, M., Busch, P. and Park, Y. (2017) Homo-trimerization is essential for the transcription factor function of Myrf for oligodendrocyte differentiation. *Nucleic Acids Res.*, **45**, 5112–5125.

21. Bujalka, H., Koenning, M., Jackson, S., Perreau, V.M., Pope, B., Hay, C.M., Mitew, S., Hill, A.F., Lu, Q.R., Wegner, M. et al. (2013) MYRF is a membrane-associated transcription factor that autoproteolytically cleaves to directly activate myelin genes. *Plos Biol.*, **11**, e1001625.

22. Choi, J.-o., Fan, C., Kim, D., Sharif, M., An, H. and Park, Y. (2018) Elucidating the transactivation domain of the pleiotropic transcription factor Myrf. *Sci. Rep.*, **8**, 13075.

23. Emery, B., Agalliu, D., Cahoy, J.D., Watkins, T.A., Dugas, J.C., Mulinyawe, S.B., Ibrahim, A., Ligon, K.L., Rowitch, D.H. and Barres, B.A. (2009) Myelin gene regulatory factor is a critical transcriptional regulator required for CNS myelination. *Cell*, **138**, 172–185.

24. McKenzie, I.A., Ohayon, D., Li, H., de Faria, J.P., Emery, B., Tohyama, K. and Richardson, W.D. (2014) Motor skill learning requires active central myelination. *Science*, **346**, 318–322.

25. Yu, Y., Chen, Y., Kim, B., Wang, H., Zhao, C., He, X., Liu, L., Liu, W., Wu, L.M.N., Mao, M. et al. (2013) Olig2 targets chromatin remodelers to enhancers to initiate oligodendrocyte differentiation. *Cell*, **152**, 248–261.

26. Bischof, M., Weider, M., Küspert, M., Nave, K.-A. and Wegner, M. (2015) Brg1-dependent chromatin remodelling is not essentially required during oligodendroglial differentiation. *J. Neurosci.*, **35**, 21–35.

27. He, D., Marie, C., Zhao, C., Kim, B., Wang, J., Deng, Y., Clavairoly, A., Frah, M., Wang, H., He, X. et al. (2016) Chd7 cooperates with Sox10 and regulates the onset of CNS myelination and remyelination. *Nat. Neurosci.*, **19**, 678–689.

28. Stolt, C.C., Rehberg, S., Ader, M., Lommes, P., Riethmacher, D., Schachner, M., Bartsch, U. and Wegner, M. (2002) Terminal differentiation of myelin-forming oligodendrocytes depends on the transcription factor Sox10. *Genes Dev.*, **16**, 165–170.

29. Hammond, E., Lang, J., Maeda, Y., Pleasure, D., Angus-Hill, M., Xu, J., Horiuchi, M., Deng, W. and Guo, F. (2015) The Wnt effector transcription factor 7-like 2 positively regulates oligodendrocyte differentiation in a manner independent of Wnt/β-catenin signaling. *J. Neurosci.*, **35**, 5007–5022.

30. Zhao, C., Deng, Y., Liu, L., Yu, K., Zhang, L., Wang, H., He, X., Wang, J., Lu, C., Wu, L.N. et al. (2016) Dual regulatory switch through interactions of Tcf7l2/Tcf4 with stage-specific partners propels oligodendroglial maturation. *Nat. Commun.*, **7**, 10883.

31. Lopez-Anido, C., Sun, G., Koenning, M., Srinivasan, R., Hung, H.A., Emery, B., Keles, S. and Svaren, J. (2015) Differential Sox10 genomic occupancy in myelinating glia. *Glia*, **63**, 1897–1914.

32. Dixon, J.R., Selvaraj, S., Yue, F., Kim, A., Li, Y., Shen, Y., Hu, M., Liu, J.S. and Ren, B. (2012) Topological domains in mammalian genomes identified by analysis of chromatin interactions. *Nature*, **485**, 376–380.

33. Rao, S.S., Huntley, M.H., Durand, N.C., Stamenova, E.K., Bochkov, I.D., Robinson, J.T., Sanborn, A.L., Machol, I., Omer, A.D., Lander, E.S. et al. (2014) A 3D map of the human genome at kilobase resolution reveals principles of chromatin looping. *Cell*, **159**, 1665–1680.

34. Nora, E.P., Dekker, J. and Heard, E. (2013) Segmental folding of chromosomes: a basis for structural and regulatory chromosomal neighborhoods? *Bioessays*, **35**, 818–828.

35. Pope, B.D., Ryba, T., Dileep, V., Yue, F., Wu, W., Denas, O., Vera, D.L., Wang, Y., Hansen, R.S., Canfield, T.K. et al. (2014) Topologically associating domains are stable units of replication-timing regulation. *Nature*, **515**, 402–405.

36. Dixon, J.R., Jung, I., Selvaraj, S., Shen, Y., Antosiewicz-Bourget, J.E., Lee, A.Y., Ye, Z., Kim, A., Rajagopal, N., Xie, W. et al. (2015) Chromatin architecture reorganization during stem cell differentiation. *Nature*, **518**, 331–336.

37. Flavahan, W.A., Drier, Y., Liau, B.B., Gillespie, S.M., Venteicher, A.S., Stemmer-Rachamimov, A.O., Suvà, M.L. and Bernstein, B.E. (2016) Insulator dysfunction and oncogene activation in IDH mutant gliomas. *Nature*, **529**, 110–114.

38. Gilbert, L.A., Horlbeck, M.A., Adamson, B., Villalta, J.E., Chen, Y., Whitehead, E.H., Guimaraes, C., Panning, B., Ploegh, H.L., Bassik, M.C. et al. (2014) Genome-scale CRISPR-mediated control of gene repression and activation. *Cell*, **159**, 647–661.

39. Horlbeck, M.A., Gilbert, L.A., Villalta, J.E., Adamson, B., Pak, R.A., Chen, Y., Fields, A.P., Park, C.Y., Corn, J.E., Kampmann, M. *et al.* (2016) Compact and highly active next-generation libraries for CRISPR-mediated gene repression and activation. *eLife*, **5**, e19760.

40. Kearns, N.A., Pham, H., Tabak, B., Genga, R.M., Silverstein, N.J., Garber, M. and Maehr, R. (2015) Functional annotation of native enhancers with a Cas9-histone demethylase fusion. *Nat. Methods*, **12**, 401–403.

41. Thakore, P.I., D'Ippolito, A.M., Song, L., Safi, A., Shivakumar, N.K., Kabadi, A.M., Reddy, T.E., Crawford, G.E. and Gersbach, C.A. (2015) Highly specific epigenome editing by CRISPR-Cas9 repressors for silencing of distal regulatory elements. *Nat. Methods*, **12**, 1143–1149.

42. Fulco, C.P., Munschauer, M., Anyoha, R., Munson, G., Grossman, S.R., Perez, E.M., Kane, M., Cleary, B., Lander, E.S. and Engreitz, J.M. (2016) Systematic mapping of functional enhancer–promoter connections with CRISPR interference. *Science*, **354**, 769–773.

43. Klann, T.S., Black, J.B., Chellappan, M., Safi, A., Song, L., Hilton, I.B., Crawford, G.E., Reddy, T.E. and Gersbach, C.A. (2017) CRISPR–Cas9 epigenome editing enables high-throughput screening for functional regulatory elements in the human genome. *Nat. Biotechnol.*, **35**, 561–568.

44. Jung, M., Krämer, E., Grzenkowski, M., Tang, K., Blakemore, W., Aguzzi, A., Khazaie, K., Chlichlia, K., von Blankenfeld, G., Kettenmann, H. *et al.* (1995) Lines of murine oligodendroglial precursor cells immortalized by an activated neu tyrosine kinase show distinct degrees of interaction with axons in vitro and in vivo. *Eur. J. Neurosci.*, **7**, 1245–1265.

45. Gong, Y., Lazaris, C., Sakellaropoulos, T., Lozano, A., Kambadur, P., Ntziachristos, P., Aifantis, I. and Tsirigos, A. (2018) Stratification of TAD boundaries reveals preferential insulation of super-enhancers by strong boundaries. *Nat. Commun.*, **9**, 542.

46. Cusanovich, D.A., Hill, A.J., Aghamirzaie, D., Daza, R.M., Pliner, H.A., Berletch, J.B., Filippova, G.N., Huang, X., Christiansen, L., DeWitt, W.S. *et al.* (2018) A single-cell atlas of in vivo mammalian chromatin accessibility. *Cell*, **174**, 1309–1324.

47. Badea, T.C., Niculescu, F.I., Soane, L., Shin, M.L. and Rus, H. (1998) Molecular cloning and characterization of RGC-32, a novel gene induced by complement activation in oligodendrocytes. *J. Biol. Chem.*, **273**, 26977–26981.

48. Huang, W.-Y., Li, Z.-G., Rus, H., Wang, X., Jose, P.A. and Chen, S.-Y. (2009) RGC-32 mediates transforming growth factor-β-induced epithelial-mesenchymal transition in human renal proximal tubular cells. *J. Biol. Chem.*, **284**, 9426–9432.

49. Tegla, C.A., Cudrici, C.D., Azimzadeh, P., Singh, A.K., Trippe, R., Khan, A., Chen, H., Andrian-Albescu, M., Royal, W., Bever, C. *et al.* (2013) Dual role of response gene to complement-32 in multiple sclerosis. *Exp. Mol. Pathol.*, **94**, 17–28.

50. Doi, T., Ogata, T., Yamauchi, J., Sawada, Y., Tanaka, S. and Nagao, M. (2017) Chd7 collaborates with Sox2 to regulate activation of oligodendrocyte precursor cells after spinal cord injury. *J. Neurosci.*, **37**, 10290–10309.

51. Zhang, Y., Chen, K., Sloan, S.A., Bennett, M.L., Scholze, A.R., O'Keeffe, S., Phatnani, H.P., Guarnieri, P., Caneda, C., Ruderisch, N. *et al.* (2014) An RNA-sequencing transcriptome and splicing database of glia, neurons, and vascular cells of the cerebral cortex. *J. Neurosci.*, **34**, 11929–11947.

52. Liu, J. and Casaccia, P. (2010) Epigenetic regulation of oligodendrocyte identity. *Trends Neurosci.*, **33**, 193–201.

53. Mitew, S., Hay, C.M., Peckham, H., Xiao, J., Koenning, M. and Emery, B. (2014) Mechanisms regulating the development of oligodendrocytes and central nervous system myelin. *Neuroscience*, **276**, 29–47.

54. Li, Z., Xie, W.-B., Escano, C.S., Asico, L.D., Xie, Q., Jose, P.A. and Chen, S.-Y. (2011) Response gene to complement 32 is essential for fibroblast activation in renal fibrosis. *J. Biol. Chem.*, **286**, 41323–41330.

55. Cui, X.-B., Luan, J.-N., Dong, K., Chen, S., Wang, Y., Watford Wendy, T. and Chen, S.-Y. (2018) RGC-32 (response gene to complement 32) deficiency protects endothelial cells from inflammation and attenuates atherosclerosis. *Arterioscler. Thromb. Vasc. Biol.*, **38**, e36–e47.

56. Kowarz, E., Löscher, D. and Marschalek, R. (2015) Optimized sleeping beauty transposons rapidly generate stable transgenic cell lines. *Biotechnol. J.*, **10**, 647–653.

57. Durand, N.C., Robinson, J.T., Shamim, M.S., Machol, I., Mesirov, J.P., Lander, E.S. and Aiden, E.L. (2016) Juicebox provides a visualization system for Hi-C contact maps with unlimited zoom. *Cell Sys.*, **3**, 99–101.